Semi-analytical investigation of stress interfacial effects in ductile media with nanosized spheroidal cavities

Vincent Monchiet, D. Kondo

Semi-analytical investigation of stress interfacial effects in ductile media with nanosized spheroidal cavities

Vincent MONCHIET [a], Djimedo KONDO [b]

[a] *Université Paris-Est, Modélisation et Simulation Multi Echelle, MSME UMR 8208 CNRS,*
5 bd Descartes, 77454 Marne-la-Vallée, France

[b] *Université Pierre et Marie Curie, Institut D'Alembert, UMR 7190 CNRS,*
4, Place Jussieu, 75252 Paris Cedex 05, France

Abstract

In this paper we investigate the interfacial stress effects on the macroscopic yield strength of plastic porous media containing nanosized spheroidal cavities. The solid matrix is assumed to obey the von Mises criterion with associated flow rule. Analysis of a rigid-ideal plastic spheroidal unit cell, containing a confocal spheroidal cavity, and subjected to arbitrary mechanical loadings is made. Void size effects are captured by considering at the interface between the matrix and the cavity a surface stress model, which relates the jump of the traction vector to the interfacial residual stress and to interfacial plastic strain. The resulting macroscopic criterion for the nanoporous material exhibits unusual features such as (i) an increase of the yield stress when the void size is decreased, (ii) asymmetry between the yield stress in uniaxial tension and compression.

Key words: Ductile Materials, Yield Criterion, Size effect, Spheroidal Voids, Interfacial Stress.

1 Introduction

The elastic properties of a solid are significantly affected by the presence of surfaces and interfaces (see [24,2] for experimental evidence and [19,3] for numerical results). Surface effects are attributed to the presence of few layers

Email addresses: vincent.monchiet@univ-mlv.fr (Vincent MONCHIET), djimedo.kondo@upmc.fr (Djimedo KONDO).

of atoms which experience a different local environment than atoms in the bulk and have a different equilibrium positions and energy. The classic three-dimensional linear-elasticity theory generally neglects these effects since the considered objects and structural elements are, at less, microsized but never of the size of one or few nanometers. For such nanosized objects, the interfacial effects become predominant since the area of surface per unit of volume is very high. Surface effects in standard continuum theories are treated within the framework of the Gurtin and Murdoch stress interface model [13] which assumes a jump of the traction vector while the displacement field is considered continuous across the surface. The jump condition may comply with a generalized Young-Laplace equation which extends to solid-solid interface the well known equation that describes capillarity effects in fluid mechanics. Thus, the discontinuity of the traction vector consists of two parts, the first one is attributed to the presence of interfacial residual stresses, independent of the deformation, and the second one being related to elastic deformation of the interface. Stress surface model have been used to model the inclusions size dependency of elastic properties of nanocomposites [7,22,15,1].

However, surface effects on the yield strength and plastic behavior of nano objects and nanostructured materials have also been observed (see for instance [18,25] for experimental evidence and [4,5,8,26] for numerical simulations). Indeed, atomistic-based simulations performed by [8] have shown that the yield stress of gold nanowires strongly increases as the cross-section decreases. Note also that [4] reports that the magnitude of the yield stress is larger in tension than in compression for very small nanowires, the authors attributing this asymmetry mainly to surface effects. Few recent studies consider stress interfaces effects in the context of non-linear composites and nanoporous plastic materials [27–29,6,11]. In particular, by performing a limit analysis of a hollow sphere, [6] generalize the Gurson model [12] in order to predict void size effects. To this end, they make use of a plastic version of the Gurtin stress interface model (see for instance [21]) which relates the interfacial stress to the plastic deformation at the cavity surface. The resulting model shows a void size dependency of the macroscopic yield strength of nanoporous media: for nanosized cavities, the strength domain appears to be significantly larger than that predicted by the Gurson model. Alternatively, non-local plasticity theories have been used in [23,14,16,17] instead of the von Mises criterion for describing the plastic behavior of the solid matrix. Yet, a major advantage of the analysis based on stress interface over non-local plasticity theories, is hat it is possible to derive closed-form expressions of the overall plastic dissipation of porous solids containing nanosized cavities. Nevertheless, in [6], the authors restrict their analysis to the case of spherical cavities. In this contribution, we provide an extension of the model presented in [6] to the case of spheroidal cavities. By doing so, we also extend the work of Gologanu et al. [9,10] by incorporating both void shape and void size effects.

2 Definition of the unit cell

Let us consider a spheroidal cavity of semi-axes a_1 and b_1 embedded in a spheroid of semi-axes a_2 and b_2. The axis of the spheroids are aligned with $0x_3$, where $(0, x_1, x_2, x_3)$ is a cartesian coordinate system of orthonormal basis $(\underline{e}_1, \underline{e}_2, \underline{e}_3)$. The volume of the cavity is $V_1 = 4\pi a_1 b_1^2/3$ while the total volume of the unit-cell is $V_2 = 4\pi a_2 b_2^2/3$. The shape of the cavity is described by the aspect ratio a_1/b_1, with $a_1 > b_1$ corresponding to a prolate cavity while $b_1 > a_1$ to an oblate one. Let us denote by c the focal distance and by e_1 the void eccentricity, defined by:

$$\begin{aligned} &c = \sqrt{a_1^2 - b_1^2} = \sqrt{a_2^2 - b_2^2} \quad e_1 = \frac{c}{a_1} \quad e_2 = \frac{c}{a_2} \quad \text{(prolate)} \\ &c = \sqrt{b_1^2 - a_1^2} = \sqrt{b_2^2 - a_2^2} \quad e_1 = \frac{c}{b_1} \quad e_2 = \frac{c}{b_2} \quad \text{(oblate)} \end{aligned} \tag{1}$$

We will use both cylindrical coordinates ρ, θ, z with $(\underline{e}_\rho, \underline{e}_\theta, \underline{e}_z)$ the associated orthonormal basis and the classical spheroidal coordinates λ, φ, θ (associated orthogonal basis $(\underline{e}_\lambda, \underline{e}_\phi, \underline{e}_\theta)$) defined by:

$$\begin{cases} x_1 = b\sin(\varphi)\cos(\theta) \\ x_2 = b\sin(\varphi)\sin(\theta) \\ x_3 = a\cos(\varphi) \end{cases} \qquad \begin{cases} \underline{e}_\lambda = \dfrac{1}{L_\lambda}\left\{a\sin(\varphi)\ \underline{e}_\rho + b\cos(\varphi)\ \underline{e}_3\right\} \\ \underline{e}_\varphi = \dfrac{1}{L_\lambda}\left\{b\cos(\varphi)\ \underline{e}_\rho - a\sin(\varphi)\ \underline{e}_3\right\} \\ \underline{e}_\theta = \underline{e}_\theta \end{cases} \tag{2}$$

with $L_\lambda = \sqrt{a^2\sin^2(\varphi) + b^2\cos^2(\varphi)}$, $\lambda \in [0, +\infty[$, $\varphi \in [0, \pi]$ and $\underline{e}_\rho = \cos(\theta)\underline{e}_1 + \sin(\theta)\underline{e}_2$, $\theta \in [0, 2\pi]$. In the above equations: $a = c\cosh(\lambda)$ and $b = c\sinh(\lambda)$ for a prolate void, while for the case of an oblate void $a = c\sinh(\lambda)$ and $b = c\cosh(\lambda)$. The iso-λ surfaces define confocal spheroids with foci $c = \sqrt{|a^2 - b^2|}$ and eccentricity $e = c/a$, for a prolate void while $e = c/b$ for an oblate one. The porosity f is defined by: $f = (a_1 b_1^2)/(a_2 b_2^2)$. The matrix of the spheroidal unit cell is made of a rigid-plastic material obeying to the von Mises yield criterion, $\sigma_{eq} \leq \sigma_0$, ($\sigma_0$ being the yield stress in tension and σ_{eq} the von Mises equivalent stress $\sigma_{eq} = \sqrt{\frac{3}{2}\boldsymbol{\sigma} : \boldsymbol{\sigma}}$) and the associated flow rule:

$$\boldsymbol{\sigma} = \frac{2\sigma_0}{3}\frac{\boldsymbol{d}}{d_{eq}}, \quad \text{with} \quad d_{eq} = \sqrt{\frac{2}{3}\boldsymbol{d} : \boldsymbol{d}}, \quad \boldsymbol{d} = \frac{1}{2}(\nabla \otimes \underline{v} + \underline{v} \otimes \nabla) \tag{3}$$

where $\underline{v}$ is the velocity field, $\boldsymbol{d}$ the strain rate tensor and d_{eq} the von Mises equivalent strain rate.

The surface between the void and the solid matrix, denoted Γ, is assumed to be described by a stress-type interface model, which was introduced by [13] in the context of elasticity and extended by [6,21] to plasticity. Stress interfaces ensure the continuity of the velocity field while the traction vector, $\underline{t} = \boldsymbol{\sigma}.\underline{n}$, undergoes a jump which is governed by the Young-Laplace equation:

$$[\underline{t}]_\Gamma = -\operatorname{div}_s(\boldsymbol{\tau}) \tag{4}$$

In the above equation, $\operatorname{div}_s(\boldsymbol{\tau})$ denotes the surface divergence of the tensor $\boldsymbol{\tau}$ such that vector $\operatorname{div}_s(\boldsymbol{\tau}) = (\boldsymbol{\tau} \otimes \underline{\nabla}) : \boldsymbol{P}(\underline{n})$, with $\boldsymbol{P}(\underline{n}) = \boldsymbol{I} - \underline{n} \otimes \underline{n}$, $\boldsymbol{I}$ being the second order identity tensor and $\underline{n}$ the normal unit vector taken on the interface Γ and oriented from the void to the solid matrix. In (4), the notation $[\underline{t}]_\Gamma$ represents the jump of $\underline{t}$ across Γ defined as follows: $[\underline{t}]_\Gamma = \underline{t}^+ - \underline{t}^-$, where $\underline{t}^+$ and $\underline{t}^-$ are the values of the traction vector calculated on both sides of Γ. When the interface Γ is the bounday between a void and a solid, $\underline{t}^- = 0$ and relation (4) reduces to $\underline{t}^+ = -\operatorname{div}_s(\boldsymbol{\tau})$.
In equation (4), the interfacial stress, $\boldsymbol{\tau}$, is given by:

$$\boldsymbol{\tau} = \tau_r \boldsymbol{P}(\underline{n}) + \frac{2\tau_0}{3d^s_{eq}}(\boldsymbol{d}_s + \operatorname{tr}(\boldsymbol{d}_s)\boldsymbol{P}(\underline{n})) \tag{5}$$

where τ_r is the interfacial residual stress, τ_0 is a material parameter and $\boldsymbol{d}_s$ is the interfacial plastic strain rate which is defined as the restriction of the total strain rate to the tangent plane of normal unit vector $\underline{n}$. In (5), d^s_{eq} is the surface equivalent strain rate. The expressions of $\boldsymbol{d}^s$ and d^s_{eq} are:

$$\begin{aligned} \boldsymbol{d}_s &= \boldsymbol{P}(\underline{n}).\boldsymbol{d}.\boldsymbol{P}(\underline{n}) \\ d^s_{eq} &= \left[\frac{2}{3}\left(\boldsymbol{d}_s : \boldsymbol{d}_s + \operatorname{tr}(\boldsymbol{d}_s)^2\right)\right]^{1/2} \end{aligned} \tag{6}$$

Note that for a spheroidal surface $\underline{n} = \underline{e}_\lambda$, $\boldsymbol{P}(\underline{n}) = \underline{e}_\theta \otimes \underline{e}_\theta + \underline{e}_\varphi \otimes \underline{e}_\varphi$ and the quantities $\boldsymbol{d}_s$ and d^s_{eq} read:

$$\begin{aligned} \boldsymbol{d}_s &= d_{\theta\theta}\underline{e}_\theta \otimes \underline{e}_\theta + d_{\varphi\varphi}\underline{e}_\varphi \otimes \underline{e}_\varphi + d_{\theta\varphi}(\underline{e}_\theta \otimes \underline{e}_\varphi + \underline{e}_\varphi \otimes \underline{e}_\theta) \\ d^s_{eq} &= \left[\frac{4}{3}(d^2_{\theta\theta} + d^2_{\varphi\varphi} + d^2_{\theta\varphi} + d_{\theta\theta}d_{\varphi\varphi})\right]^{1/2} \end{aligned} \tag{7}$$

3 Limit analysis taking into consideration interfacial stresses

As already mentioned, Hill-Mandel kinematic homogenization approach will be used to derive the overall plastic potential of the porous solid. Thus, uniform strain rate boundary conditions are considered on external surface of the hollow spheroid:

$$\underline{v}(\lambda = \lambda_2) = \boldsymbol{D}.\underline{x} \tag{8}$$

where $\boldsymbol{D}$ is the macroscopic strain rate tensor.

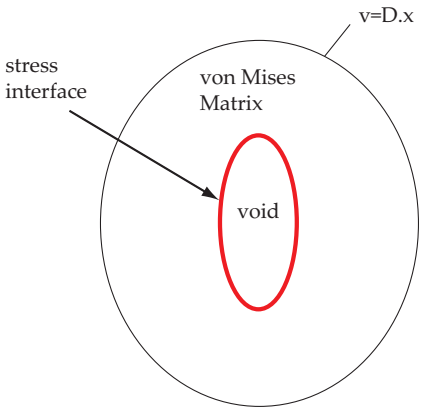

Fig. 1. Schematic diagram showing the hollow spheroid with a stress interface.

The limit stress at the macroscopic scale, $\boldsymbol{\Sigma}$, is:

$$\boldsymbol{\Sigma} = \frac{\partial \Pi}{\partial \boldsymbol{D}}(\boldsymbol{D}) \tag{9}$$

where $\Pi(\boldsymbol{D})$, is the macroscopic dissipation given by:

$$\Pi(\boldsymbol{D}) = \inf_{\underline{v} \in \mathcal{K}} \frac{1}{V_2} \left[\int_{\Omega - \omega} \sigma_0 d_{eq} dV + \int_{\Gamma} [\underline{t}]_{\Gamma} . \underline{v} dS \right] \tag{10}$$

where $\mathcal{K}$ is the space of admissible velocity fields, i.e. of continuous and differentiable velocity fields that comply with condition (8). The first integral in (10) is computed over the solid matrix, defined by $\Omega - \omega$, where Ω is the domain corresponding to the unit cell, while ω is the domain occupied by the void. The second integral in (10) is performed over the surface Γ of the void. It is recalled that $V_2 = 4\pi a_2 b_2^2/3$ is the volume of Ω. Using the generalized Young-Laplace equation (4), it is readily seen that the second integral is related to the interfacial residual stress and interfacial plastic strain. It then follows that:

$$\int_\Gamma [\underline{t}]_\Gamma .\underline{v} dS = -\int_\Gamma \mathrm{div}_s(\boldsymbol{\tau}).\underline{v} dS \tag{11}$$

Moreover, for any continuously differentiable second order tensor $\boldsymbol{\tau}$ and vector $\underline{v}$,

$$\mathrm{div}_s(\boldsymbol{\tau}.\underline{v}) = \mathrm{div}_s(\boldsymbol{\tau}).\underline{v} + \boldsymbol{\tau} : \boldsymbol{d}_s \tag{12}$$

The integral over Γ of the quantity $\mathrm{div}_s(\boldsymbol{\tau}.\underline{v})$ being null over any closed surface, it follows that:

$$\int_\Gamma \mathrm{div}_s(\boldsymbol{\tau}).\underline{v} dS = -\int_\Gamma \boldsymbol{\tau} : \boldsymbol{d}_s dS \tag{13}$$

Finally, replacing $\boldsymbol{\tau}$ by its expression (5), one obtains:

$$\Pi(\boldsymbol{D}) = \inf \left[\frac{1}{V_2} \int_{\Omega-\omega} \sigma_0 d_{eq} dV + \frac{1}{V_2} \int_\Gamma \tau_0 d^s_{eq} dS + \frac{1}{V_2} \int_\Gamma \tau_r \,\mathrm{tr}(\boldsymbol{d}^s) dS \right] \tag{14}$$

Note that this expression of $\Pi(\boldsymbol{D})$ contains three terms: the first is classic in the context of Limit Analysis of ductile porous media; the last two terms are associated to interfacial plastic dissipations.
Note that, in the spheroidal coordinate system, the surface integral is defined by:

$$\int_\Gamma \bullet \; dS = \int_{\varphi=0}^{\varphi=\pi} \int_{\theta=0}^{\theta=2\pi} \bullet \; b_1 L_{\lambda_1} \sin(\varphi) d\varphi d\theta \tag{15}$$

where L_{λ_1} is the value of L_λ for $\lambda = \lambda_1$, i.e. $L_{\lambda_1} = \sqrt{a_1^2 \sin^2(\varphi) + b_1^2 \cos^2(\varphi)}$; for the definition of the volume integral in the expression of $\Pi(\boldsymbol{D}$, the reader is referred to [9,10].

4 The trial velocity field

A crucial step in the derivation of an approximate closed form expression of the macroscopic potential of the ductile porous material lies in the choice of the trial velocity field. Generally, this field is composed in two parts: one involving a constant traceless tensor $\boldsymbol{A}$, one, denoted $\underline{v}^E$, which is heterogeneous, i.e.

$$\underline{v} = \boldsymbol{A}.\underline{x} + B\underline{v}^E \tag{16}$$

Due to additional difficulties related to the consideration of interfacial stress effects, we propose here to adopt, for $\underline{v}^E$, the velocity field considered by Gologanu et al. [9,10] and Monchiet et al. [20]. This field has the property to comply with uniform strain rate conditions on any iso-$\lambda = cst$ spheroid. Its expression is:

$$\begin{cases} v_\lambda^E = \dfrac{c^3}{bL_\lambda}\left[1 + \dfrac{1}{2}(1-3\alpha)(1-3\cos^2(\varphi))\right] \\ v_\varphi^E = \dfrac{3c^3}{4ab^2L_\lambda}[(1-\alpha)b^2 - 2\alpha a^2]\sin(2\varphi) \\ v_\theta^R = 0 \end{cases} \tag{17}$$

where α depends on λ or equivalently on e and is given by:

$$\alpha = \begin{cases} \dfrac{ab^2}{c^3}\operatorname{arctanh}\left\{\dfrac{c}{a}\right\} - \dfrac{b^2}{c^2} & \text{(prolate void)} \\ -\dfrac{ab^2}{c^3}\arctan\left\{\dfrac{c}{a}\right\} + \dfrac{b^2}{c^2} & \text{(oblate void)} \end{cases} \tag{18}$$

For the explicit dependence of a and b on the coordinates λ and e, the reader is referred to section 2.
The verification of uniform strain rate boundary conditions at the outer spheroid $\lambda = \lambda_2$ leads to:

$$\boldsymbol{A} = \boldsymbol{D} - D_m\boldsymbol{T}; \qquad B = \frac{a_2b_2^2}{c^3}D_m \tag{19}$$

where the second order tensor $\boldsymbol{T}$ is given by:

$$\boldsymbol{T} = \frac{3}{2}(1-\alpha)(\underline{e}_1 \otimes \underline{e}_1 + \underline{e}_2 \otimes \underline{e}_2) + 3\alpha\underline{e}_3 \otimes \underline{e}_3 \tag{20}$$

From equation (17), it is readily seen that the strain rate field in the matrix is the sum of a homogenous deviatoric field $\boldsymbol{A}$ and a non-homogeneous field $\boldsymbol{d}^E$:

$$\boldsymbol{d} = \boldsymbol{A} + B\boldsymbol{d}^E \tag{21}$$

with $\boldsymbol{d}^E$ given by:

$$\begin{cases} d^E_{\lambda\lambda} = -\dfrac{3c^3}{ab^2}(1-\alpha) + \dfrac{3c^3 a}{2b^2 L_\lambda^2}(1-3\alpha)\sin^2(\varphi) \\ d^E_{\varphi\varphi} = \dfrac{3c^3}{2ab^2}(1-\alpha) - \dfrac{3c^3 a}{2b^2 L_\lambda^2}(1-3\alpha)\sin^2(\varphi) \\ d^E_{\theta\theta} = \dfrac{3c^3}{2ab^2}(1-\alpha) \\ d^E_{\lambda\varphi} = \dfrac{3c^3}{4bL_\lambda^2}(1-3\alpha)\sin(2\varphi) \end{cases} \tag{22}$$

For application purpose, we consider axisymmetric mechanical loadings. Thus, the non-null components of the macroscopic strain rate tensor, $\boldsymbol{D}$, are $D_{11} = D_{22}$ and D_{33}. Let us denote $D_q = 2(D_{33} - D_{11})/3$. It can then be shown that the equivalent strain rates d_{eq} and d^s_{eq}, which appear in the expression of the macroscopic dissipation $\Pi(\boldsymbol{D})$ (see (14)) read:

$$\begin{aligned} d_{eq} &= \sqrt{D_q^2 + 2D_q D_m F_1(\lambda,\varphi) + D_m^2 F_2(\lambda,\varphi)} \\ d^s_{eq} &= \sqrt{D_q^2 G_1(\varphi) + 2D_q D_m G_2(\varphi) + D_m^2 G_3(\varphi)} \end{aligned} \tag{23}$$

In which, functions $F_i(\lambda,\varphi)$ and $G_i(\lambda,\varphi)$ being given by:

$$\begin{cases} F_1(\lambda,\varphi) = -(z_2 + 3u(\alpha - w^2)), \\ F_2(\lambda,\varphi) = z_2^2 + 6z_2 u(\alpha - w^2) + 3u^2\Big[1 + 3\alpha^2 + 2(1-3\alpha)w^2\Big], \\ G_1(\varphi) = 1 - 3w^2 + 3w^4, \\ G_2(\varphi) = \dfrac{1}{f}\Big[(1-3w^2) - (1-3w^2+3w^4)\Delta\Big], \\ G_3(\varphi) = \dfrac{1}{f^2}\Big[4 - 2(1-3w^2)\Delta + (1-3w^2+3w^4)\Delta^2\Big] \end{cases} \tag{24}$$

with:

$$\begin{aligned} &u = \frac{a_2 b_2^2}{ab^2}, \qquad w = \frac{b\cos(\varphi)}{L_\lambda} \\ &\Delta = z_1 - f z_2, \qquad z_1 = 1 - 3\alpha_1, \qquad z_2 = 1 - 3\alpha_2 \end{aligned} \tag{25}$$

The invariants of the macroscopic stresses at yielding are:

$$\begin{cases} \Sigma_m = \dfrac{1}{3}\dfrac{\partial \Pi}{\partial D_m} \\ \Sigma_q = \dfrac{\partial \Pi}{\partial D_q} \end{cases} \tag{26}$$

where $\Sigma_m = \mathrm{tr}(\boldsymbol{\Sigma}/3 = (2\sigma_{11} + \Sigma_{33})/3$ and $\Sigma_q = \Sigma_{33} - \Sigma_{11}$ (see equation (14) for the expression of $\Pi(\boldsymbol{D})$ and (23) to (25) for d_eq and d_{seq}). Thus, the macroscopic criterion is obtained by computing numerically the three integrals in equation (14).

5 Results

In this section, we propose to illustrate the salient features of the new model, namely the effects of the void size on the macroscopic yield strength of the ductile material containing spheroidal nanocavities, in this section we present projections of the developed analytic macroscopic criterion in the deviatoric plane. As mentioned above, axisymmetric loadings are considered; the stress invariants being $\Sigma_q = \Sigma_{33} - \Sigma_{11}$ and $\Sigma_m = (2\Sigma_{11} + \Sigma_{33})/3$.

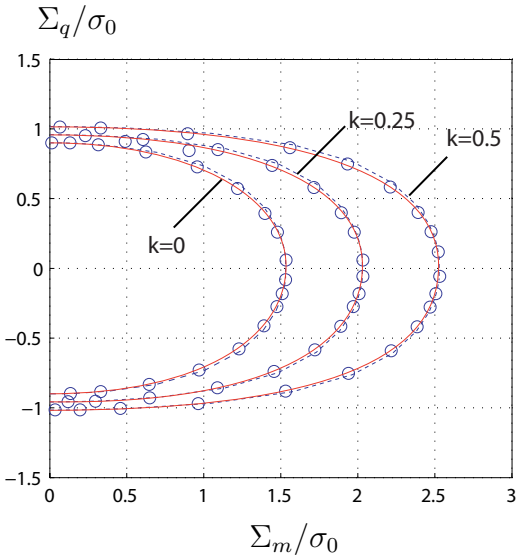

Fig. 2. Yield loci for spherical nanovoids. Comparison between the upper bound of [6] (dashed line) and the exact, numerical two-field criteria (full line with circles) for a porosity $f = 0.1$ and for various values of $k = \tau_0/(b_1\sigma_0)$.

We first consider the limiting case of spherical nano-cavities. In figure 2, we compare the predictions obtained by numerically evaluating the integral (14) with that obtained with the approximate criterion [6] for various values of the non dimensional parameter $k = \tau_0/(b_1\sigma_0)$ and fixed porosity $f = 0.1$ (τ_r,

being considered null). Clearly, the results shows an important effect of the the cavity size on the macroscopic yield locus, the yield surface being larger when the parameter $k = \tau_0/(a\sigma_0)$ increases, this corresponding to a decrease of the size of the void.
Note the very good agreement between the approximate criterion of Dormieux-Kondo [6] and the numerical results. One reason is that the trial velocity field used by [6] is the one already used by Gurson [12] to which the trial velocity field (Eq. (16) with (17)) reduces in the case of spherical cavities. Thus, the numerical results validate the approximations used in [6] by these authors. In the particular case $k = 0$, the criterion [6] reduces to Gurson's one. This is physically sound, since for large values of the cavity radius the term related to the interfacial stress vanishes.

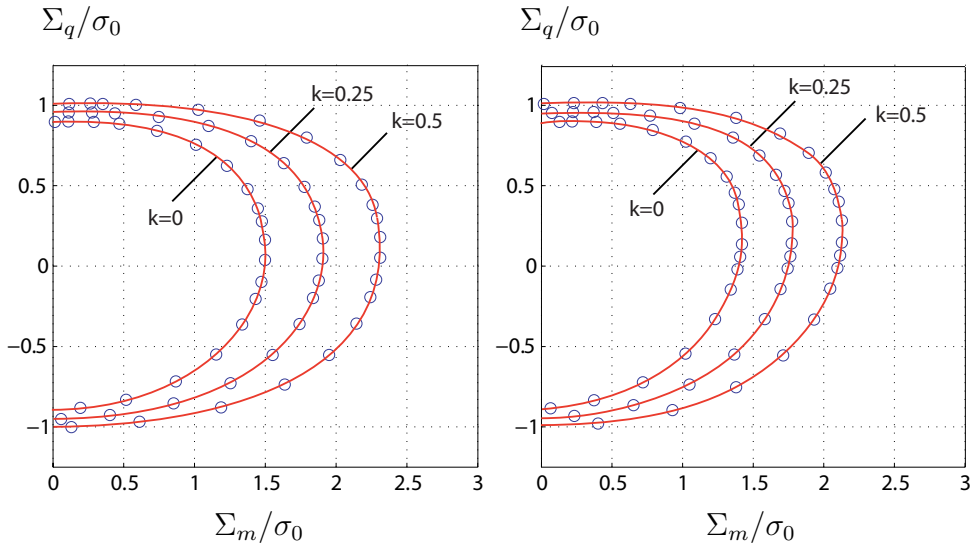

Fig. 3. Yield loci for a prolate cavity with an aspect ratio $a_1/b_1 = 2$ (at the left) $a_1/b_1 = 5$ (at the right) and a porosity $f = 0.1$.

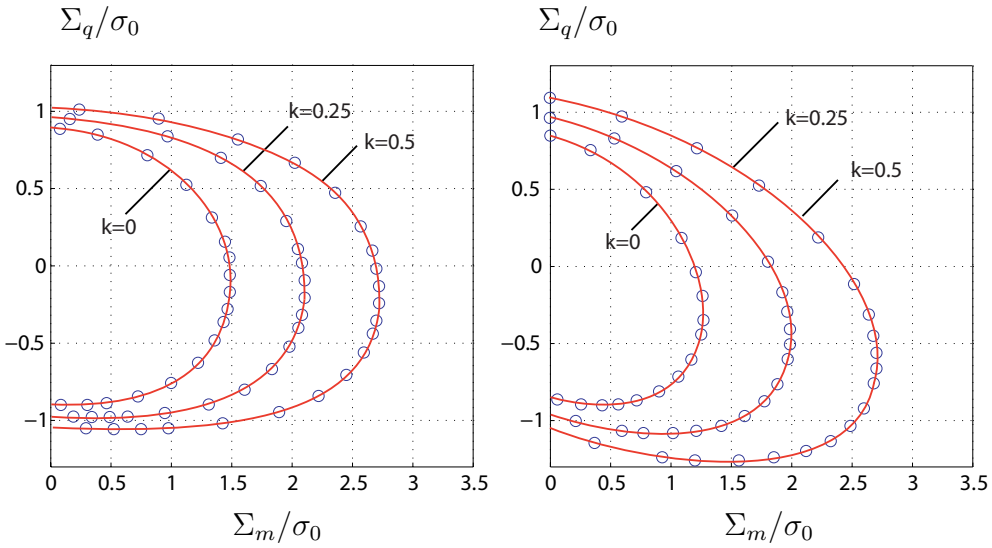

Fig. 4. Yield loci for an oblate cavity with an aspect ratio $a_1/b_1 = 1/2$ (at the left) $a_1/b_1 = 1/5$ (at the right) and a porosity $f = 0.1$.

On figure 3 is represented the yield surface for the case of a prolate cavity. On the left, the macroscopic yield surface corresponds to cavities having an aspect ratio $a_1/b_1 = 2$ while at the right, similar results are provided for the aspect ratio $a_1/b_1 = 5$. The porosity $f = 0.1$ is considered and various values of the non dimensional parameter $k = \tau_0/(b_1\sigma_0)$ are taken (the interfacial residual stress τ_r is still considered as zero). Figure 4 displays similar results for the case of an oblate cavity. At the right, the aspect ratio is $a_1/b_1 = 1/2$ while at the left, the aspect ratio is $a_1/b_1 = 1/5$. As for the case of a spherical void, the surface effect induce an increase of the resistance surface of the ductile porous medium with nano spheroidal cavities. It must be also noted that the size effect seems to be more significant in the case of an oblate cavity than for a prolate one (particularly for the aspect ratio $a_1/b_1 = 1/5$). The reason is that, for the same volume, the area of the void surface is greater for an oblate cavity than for a prolate one.

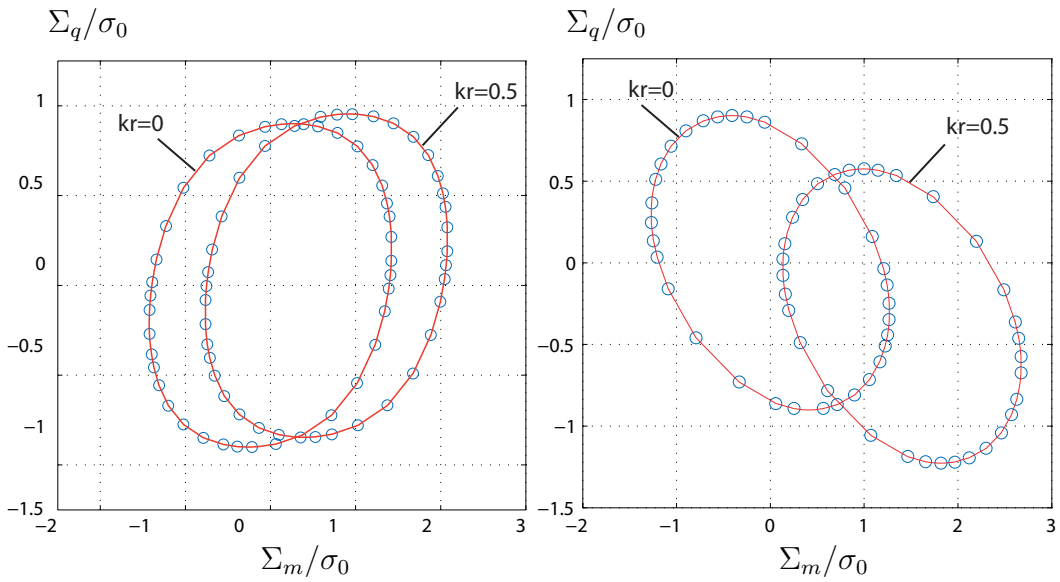

Fig. 5. Yield loci for a prolate cavity with an aspect ratio $a_1/b_1 = 5$ (at the left) for an oblate cavity with $a_1/b_1 = 1/5$ (at the right) and a porosity $f = 0.1$ and for two values of the parameter $k_r = \tau_r/(b_1\sigma_0)$.

For completeness, we now propose to evaluate the effect of the interfacial residual stresses on the macroscopic yield surface of nanoporous materials. On figure 5, at the left, are represented the surfaces of resistance for a prolate cavity with the aspect ratio $a_1/b_1 = 1/2$, a porosity $f = 0.1$ and two values for the non dimensional parameter $k_r = \tau_r/(b_1\sigma_0)$. At the right, are represented similar results for the case of an oblate cavity having the aspect ratio $a_1/b_1 = 1/5$. A significant influence of the residual stress on the yield strength of ductile porous media with nanosized spheroidal cavities is observed. More precisely, that residual stresses induce a translation of the center of the macroscopic yield surface along both axis related to the macroscopic stress invariants Σ_m and Σ_q. This imply an asymmetry of the macroscopic yield strength between tension and compression. Again, it is observed that the interfacial stress effects more pronounced for an oblate cavities than for a prolate one (and for the same reasons that one already mentioned above).

6 Conclusion

In this study the combined effects of void shape and size on yielding of the porous aggregate were investigated. To this end we have performed the limit analysis of a spheroidal unit cell made up of a von Mises solid matrix containing a confocal spheroidal cavity and a stress interface which induce a jump of the traction vector across the surface of the void. That surface effects are considered with the plastic version of the Gurtin model [21]. In the latter,

the jump of the traction vector at the void-matrix interface results from two contributions: : surface residual stresses and plastic strain rates that occurs at the surface of the void. Numerical calculations, based on the trial velocity field introduced by Gologanu et al. [9,10], has been performed in order to derive an upper bound for the macroscopic yield criterion. Illustrations has been provided for various shape of the cavity and various values of the material parameters which enter into the stress interface model. That applications clearly show a significant effect of the stress interface on the macroscopic yield surface of plastic materials containing spheroidal nanocavities. First, the interfacial stress effect due to the surface plastic deformation is characterized, at the macroscopic level, by an increase of the yield strength. The interfacial residual stress induces a change in position of the macroscopic plastic surface which implies an asymmetry between tension and compression. For completeness, it must be mentioned that the surface effects on the macroscopic yield strength of nanoporous media are more significant for oblate cavities than for a prolate one.

References

[1] **S. Brisard, L. Dormieux, D. Kondo.** Hashin-Shtrikman bounds on the bulk modulus of a nanocomposite with spherical inclusions and interface effects. *Computational Materials Science*, 48(3), 589-596, 2010.

[2] **S. Cuenot, C. Frétigny, S. Demoustier-Champagne, B. Nysten.** Surface tension effect on the mechanical properties of nanomaterials measured by atomic force microscopy. *Physical Review B.* 69, 165410, 2004.

[3] **J.K. Diao, K. Gall, M.L. Dunn.** Atomistic simulation of the structure and elastic properties of gold nanowires. *Journal of the Mechanics Physics and Solids*, 52, 1935-1962, 2004.

[4] **J. Diao, K. Gall and M.L. Dunn.** Yield Strength Asymmetry in Metal Nanowires. *Nano Letters*, 4(10), 1863-1867, 2004.

[5] **J.K. Diao, K. Gall, M.L. Dunn, J.A. Zimmerman.** Atomistic simulations of the yielding of gold nanowires. *Acta Materialia*, 54, 643-653, 2006.

[6] **L. Dormieux, D. Kondo.** An extension of Gurson model incorporating stresses effects. *International Journal of Engineering Science*, 48, 575-581, 2010.

[7] **L. Duan, J. Wang, Z.P. Huang, B.L. Karihaloo** Size-dependent effective elastic constants of solids containing nano-inhomogeneities with interface stress. *Journal of the Mechanics Physics and Solids*, 53, 1574-1596, 2005.

[8] **K. Gall, J. Diao, M.L. Dunn.** The Strength of Gold Nanowires. *Nano Letters*, 4(12), 2431-2436, 2004.

[9] **M. Gologanu, J.-B. Leblond, J. Devaux.** Approximate models for ductile metals containing non-spherical voids Ű case of axisymmetric prolate ellipsoidal cavities. *Journal of the Mechanics Physics and Solids*, 41 (11), 1723-1754, 1993.

[10] **M. Gologanu, J.B. Leblond, G. Perrin, J. Devaux.** Approximate models for ductile metals containing non-spherical voids - case of axisymmetric oblate ellipsoidal cavities. *Journal of Engineering Materials and Technology*, 116, 290-297, 1994.

[11] **T. Goudarzi, R. Avazmohammadi, R. Naghdabadi.** Surface energy effects on the yield strength of nanoporous materials containing nanoscale cylindrical voids. *Mechanics of Materials*, 42(9), 852-862, 2010.

[12] **A.L. Gurson.** Continuum theory of ductile rupture by void nucleation and growth: Part I. - Yield criterion and flow rules for porous ductile media. *Journal of Engineering Materials and Technology*, 99, 2-15, 1977.

[13] **M.E. Gurtin, A.I. Murdoch.** A continuum theory of elastic material surfaces. *Archive for Rational Mechanics and Analysis*, 57, 291-323, 1975.

[14] **M. Huang, Z. Li, C. Wang.** Coupling effects of void size and void shape on the growth of prolate ellipsoidal microvoid. *Acta Mechanica Sinica*, 21, 272-277, 2005.

[15] **H. Le Quang, Q.-C. He.** Size-dependent effective thermoelastic properties of nanocomposites with spherically anisotropic phases. *Journal of the Mechanics and Physics of Solids*, 55(9), 1899-1931, 2007.

[16] **Z. Li, M. Huang.** Combined effects of void shape and void size Ű oblate spheroidal microvoid embedded in infinite non-linear solid. *International Journal of Plasticity*, 21(3), 625-650, 2005.

[17] **Z. Li, P. Steinmann.** RVE-based studies on the coupled effects of void size and void shape on yield behavior and void growth at micron scales. *International Journal of Plasticity*, 22(7), 1195-1216, 2006.

[18] **P.E. Marszalek, W.J. Greenleaf, H. Li, A.F. Oberhauser, J.M. Fernandez.** Atomic force microscopy captures quantized plastic deformation in gold nanowires. *Proceedings of the National Academy of Sciences of the United States of America*, 97, 6282, 2000.

[19] **R.E. Miller, V.B. Shenoy.** Size-dependent elastic properties of nanosized structural elements. *Nanotechnology*, 11, 139-147, 2000.

[20] **V. Monchiet, O. Cazacu, E. Charkaluk, D. Kondo.** *Approximate criteria for anisotropic metals containing non spherical voids. International Journal of Plasticity, 24, 1158-1189, 2008.*

[21] **V. Monchiet, G. Bonnet.** Interfacial models in viscoplastic composites materials. *International Journal of Engineering Science*, 48(12), 1762-1768, 2010.

[22] **P. Sharma, S. Ganti** Size-dependent Eshelby's tensor for embedded nanoinclusions incorporating surface/interface energies. *ASME Journal of Applied Mechanics*, 71, 663-671, 2004.

[23] **J. Wen, Y. Huang, K.C. Hwang, C. Liu, M. Li.** The modified Gurson model accounting for the void size effect. *International Journal of Plasticity*, 21(2), 381-395, 2005.

[24] **E.W. Wong, P.E. Sheehan, C.M. Lieber.** Nanobeam mechanics: elasticity, strength, and toughening of nanorods and nanotubes. *Science*, 277, 1971-1975, 1997.

[25] **B. Wu, A. Heidelberg, J.J. Boland.** Mechanical properties of ultrahigh-strength gold nanowires. *Nature Materials*, 4, 525-529, 2005.

[26] **Z. Yang, Z. Lu, Y.-P. Zhao.** Atomistic simulation on size-dependent yield strength and defects evolution of metal nanowires. *Computational Materials Science*, 46, 142-150, 2009.

[27] **W. Zhang, T.J. Wang.** Effect of surface energy on the yield strength of nanoporous materials. *Applied Physics Letters*, 90, 063104, 2007.

[28] **W. Zhang, T.J. Wang, X. Chen.** Effect of surface stress on the asymmetric yield strength of nanowires. *Journal of Applied Physics*, 103, 123527, 2008.

[29] **W. Zhang, T.J. Wang, X. Chen.** Effect of surface/interface stress on the plastic deformation of nanoporous materials and nanocomposites. *International Journal of Plasticity*, 26(7), 957-975, 2010.